Adaptive Filters

Adaptive filters are capable of performance superior to that of the filters discussed thus far. However, the price paid for improved filtering power is an increase in filter complexity.

Adaptive, local noise reduction filter

The simplest statistical measures of a random variable are its mean and variance, which are reasonable parameters for an adaptive filter.

The mean gives a measure of average intensity in the region over which the mean is computed, and the variance gives a measure of contrast in that region.

The response of a filter, which operates on a local region S_{xy}, at any point (x, y) is to be based on four quantities:

(a) $g(x, y)$, the value of the noisy image at (x, y);

(b) σ_η^2, the variance of the noise corrupting $f(x, y)$ to form $\mathrm{g}(x, y)$;

(c) m_L, the local mean of the pixels in S_{xy};

(d) σ_L^2, the local variance of the pixels in S_{xy}.

We want to have the following behaviours for the filter:

1. If σ_η^2 is zero, the filter should just return the value of $\mathrm{g}(x, y)$.

   This is the zero-noise case in which $\mathrm{g}(x, y)$ is equal to $f(x, y)$.

2. If the local variance, σ_L^2, is high relative to σ_η^2, the filter should return a value close to $\mathrm{g}(x, y)$.

A high local variance typically is associated with edges, which should be preserved.

3. If the two variances are equal, we want the filter to return the arithmetic mean value of the pixels in S_{xy}.

   This condition occurs when the local area has the same properties as the overall image, and local noise is to be reduced simply by averaging.

Based on these assumptions, an adaptive expression for obtaining $\hat{f}(x,y)$ may be written as

$$\hat{f}(x,y) = \mathrm{g}(x,y) - \frac{\sigma_\eta^2}{\sigma_L^2}\left[\,\mathrm{g}(x,y) - m_L\,\right]. \qquad (5.3\text{-}12)$$

The only quantity needed to be estimated is the variance of the overall noise, σ_η^2, and other parameters can be computed from the pixels in S_{xy}.

A tacit assumption in (5.3-12) is $\sigma_\eta^2 \le \sigma_L^2$, which is reasonable because S_{xy} is a subset of $\mathrm{g}(x,y)$. In practice, however, it is possible for this condition to be violated. So, a test should be performed in implementation so that the ratio is set to 1 if $\sigma_\eta^2 > \sigma_L^2$ occurs.

Example 5.4: Illustration of adaptive, local noise-reduction filtering

Figure 5.13 (a) shows an image corrupted by additive Gaussian noise of zero mean and a variance of 1000 .

Figure 5.13 (b) is the result of applying an arithmetic mean filter of size 7×7 to Figure 5.13 (a).

Figure 5.13 (c) shows the result of applying a geometric mean filter of size 7×7 to Figure 5.13 (a).

Figure 5.13 (d) shows the result of using the adaptive filter

$$\hat{f}(x,y) = \mathrm{g}(x,y) - \frac{\sigma_\eta^2}{\sigma_L^2}\left[\,\mathrm{g}(x,y) - m_L\,\right] \qquad (5.3\text{-}12)$$

with $\sigma_\eta^2 = 1000$.

a b
c d

FIGURE 5.13 (a) Image corrupted by additive Gaussian noise of zero mean and variance 1000. (b) Result of arithmetic mean filtering. (c) Result of geometric mean filtering. (d) Result of adaptive noise reduction filtering. All filters were of size 7×7.

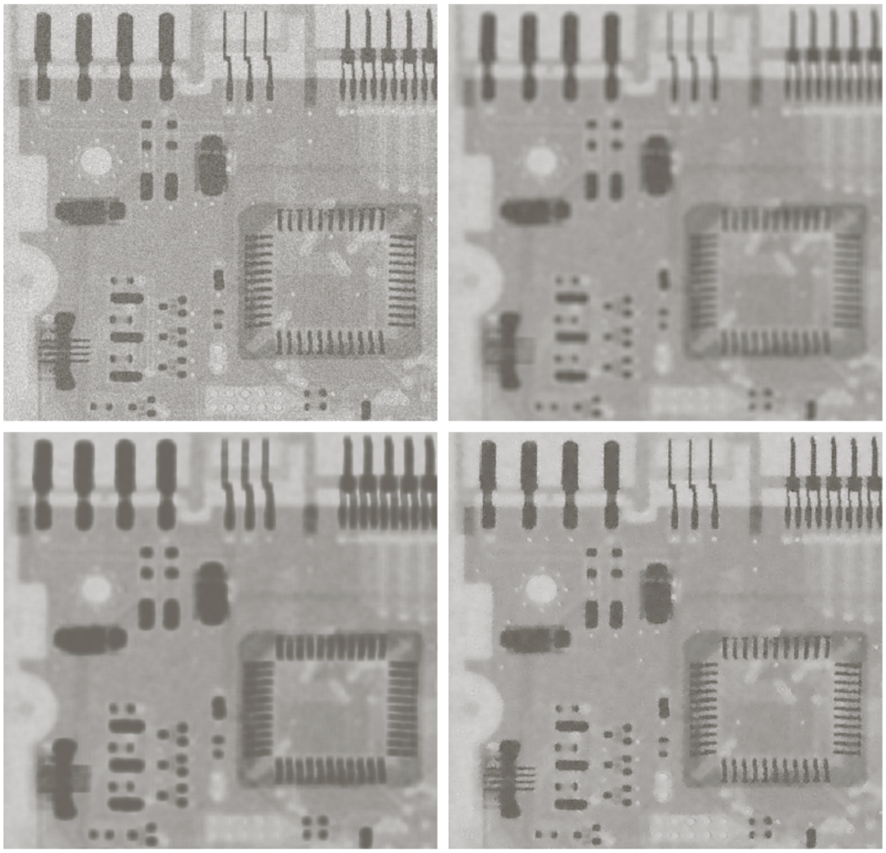

Adaptive median filter

The median filter discussed previously performs well if the spatial density of the impulse noise is not large (P_a and P_b are less than 0.2).

The adaptive median filtering can handle impulse noise with probabilities larger than these.

Unlike other filters, the adaptive median filter changes the size of S_{xy} during operation, depending on certain conditions.

Consider the following notations:

$$\begin{aligned}
z_{\min} &= \text{ minimum intensity value in } S_{xy} \\
z_{\max} &= \text{ maximum intensity value in } S_{xy} \\
z_{med} &= \text{ median of intensity values in } S_{xy} \\
z_{xy} &= \text{ intensity value at coordinates } (x,y) \\
S_{\max} &= \text{ maximum allowed size of } S_{xy}
\end{aligned}$$

The adaptive median filtering algorithm works in two stages:

```
Stage A:  A1 = $z_{med} - z_{\min}$
          A2 = $z_{med} - z_{\max}$
          If A1 $>$ 0 AND A2 $<$ 0, go to stage B
          Else increase the window size
          If window size $\leq S_{\max}$ repeat stage A
          Else output $z_{med}$

Stage B:  B1 = $z_{xy} - z_{\min}$
          B2 = $z_{xy} - z_{\max}$
          If B1 $>$ 0 AND B2 $<$ 0, output $z_{xy}$
          Else output $z_{med}$
```

Keep in mind that this algorithm has three main purposes:

to remove salt-and-pepper (impulse) noise;

to provide smoothing of other noise that may not be impulsive; and

to reduce the distortion of object boundaries.

Example 5.5: Illustration of adaptive median filtering

Figure 5.14 (a) shows an image corrupted by salt-and-pepper noise with probabilities $P_a = P_b = 0.25$.

Figure 5.14 (b) is the result of applying a 7×7 median filter. Although the noise was effectively removed, the filter caused significant loss of the detail in the image.

Figure 5.14 (c) shows the result of using the adaptive median filter with $S_{\max} = 7$. It can be observed that with the similar noise removal performance, the adaptive median filter did a better job of preserving sharpness and detail.

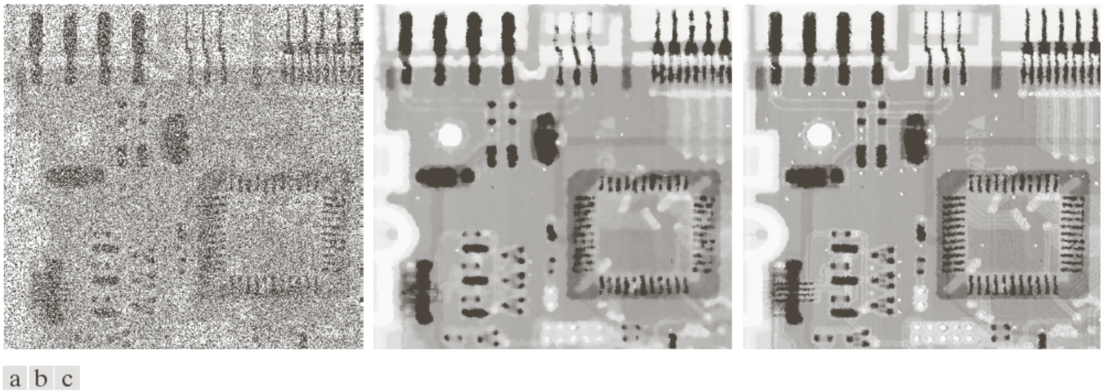

FIGURE 5.14 (a) Image corrupted by salt-and-pepper noise with probabilities $P_a = P_b = 0.25$. (b) Result of filtering with a 7×7 median filter. (c) Result of adaptive median filtering with $S_{\max} = 7$.

5.4 Periodic Noise Reduction by Frequency Domain Filtering

Periodic noise can be analyzed and filtered effectively by using frequency domain techniques.

Bandreject Filters

Figure 5.15 shows perspective plots of ideal, Butterworth, and Gaussian bandreject filters,

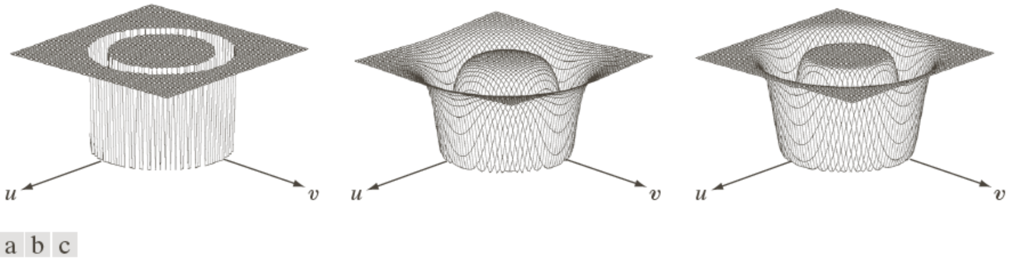

FIGURE 5.15 From left to right, perspective plots of ideal, Butterworth (of order 1), and Gaussian bandreject filters.

which were discussed in Section 4.10.1 and are summarized in Table 4.6.

TABLE 4.6
Bandreject filters. W is the width of the band, D is the distance $D(u, v)$ from the center of the filter, D_0 is the cutoff frequency, and n is the order of the Butterworth filter. We show D instead of $D(u, v)$ to simplify the notation in the table.

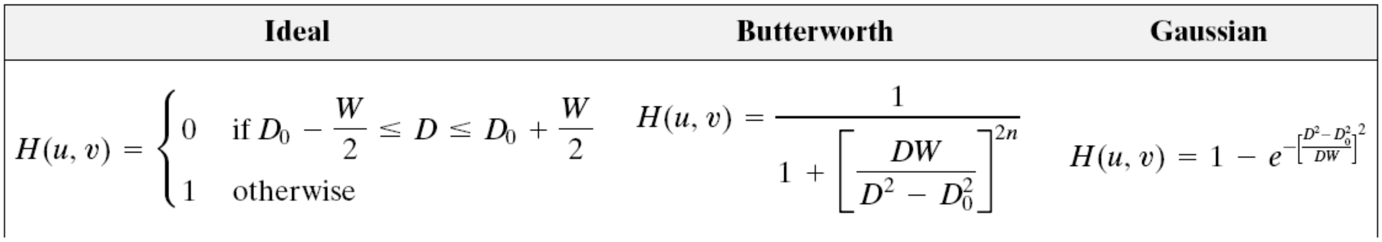

Ideal	Butterworth	Gaussian
$H(u, v) = \begin{cases} 0 & \text{if } D_0 - \frac{W}{2} \le D \le D_0 + \frac{W}{2} \\ 1 & \text{otherwise} \end{cases}$	$H(u, v) = \dfrac{1}{1 + \left[\dfrac{DW}{D^2 - D_0^2}\right]^{2n}}$	$H(u, v) = 1 - e^{-\left[\frac{D^2 - D_0^2}{DW}\right]^2}$

One of the principal applications of bandreject filtering is for noise removal in applications where the general location of the noise component(s) in the frequency domain is approximately known.

Example 5.6: Use of Bandreject filtering for periodic noise removal

Figure 5.16 (a), which is the same as Figure 5.5 (a), shows an image corrupted by sinusoidal noise of various frequencies.

The noise components can be seen as symmetric pairs of bright dots in the Fourier spectrum shown in Figure 5.16 (b).

Since the component lie on an approximate circle about the origin of the transform, so a circularly symmetric bandreject filter is a good choice.

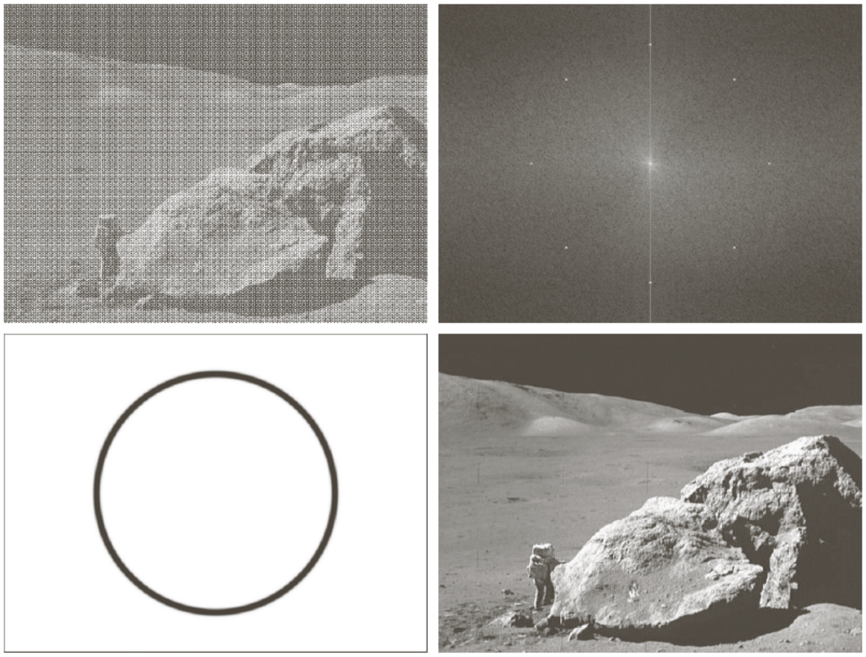

FIGURE 5.16 (a) Image corrupted by sinusoidal noise. (b) Spectrum of (a). (c) Butterworth bandreject filter (white represents 1). (d) Result of filtering. (Original image courtesy of NASA.)

Figure 5.16 (c) shows a Butterworth bandreject filter of order 4.

Figure 5.16 (d) shows the result of filtering Figure 5.16 (a) with the filter shown in Figure 5.16 (c).

Bandpass Filters

A bandpass filter performs the opposite operation of a bandreject filter.

The transfer function $H_{BP}(u,v)$ of a bandpass filter is obtained from a corresponding bandreject filter transfer function $H_{BR}(u,v)$ by using the equation

$$H_{BP}(u,v) = 1 - H_{BR}(u,v)\,. \qquad (5.4\text{-}1)$$

Performing straight bandpass filtering on an image is not a common procedure because it generally removes too much image detail. However, bandpass filtering is useful in isolating the effects on an image caused by selected frequency bands.

Example 5.7: Bandpass filtering for extracting noise patterns

The image shown in Figure 5.17 was generated by

(1) using (5.4-1) to obtain the bandpass filter corresponding to the bandreject filter used in Figure 5.16;

(2) taking the inverse transform of the bandpass-filtered transform.

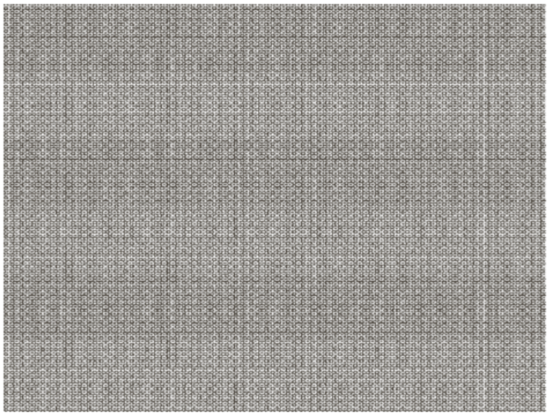

FIGURE 5.17 Noise pattern of the image in Fig. 5.16(a) obtained by bandpass filtering.

Although most image detail was lost, the remained information shows the noise pattern, which is quite close to the noise that corrupted the image in Figure 5.16.

Notch Filters

A notch filter rejects/passes frequencies in predefined neighbourhoods about a center frequency. Figure 5.18 shows plots of ideal, Butterworth, and Gaussian notch (reject) filters.

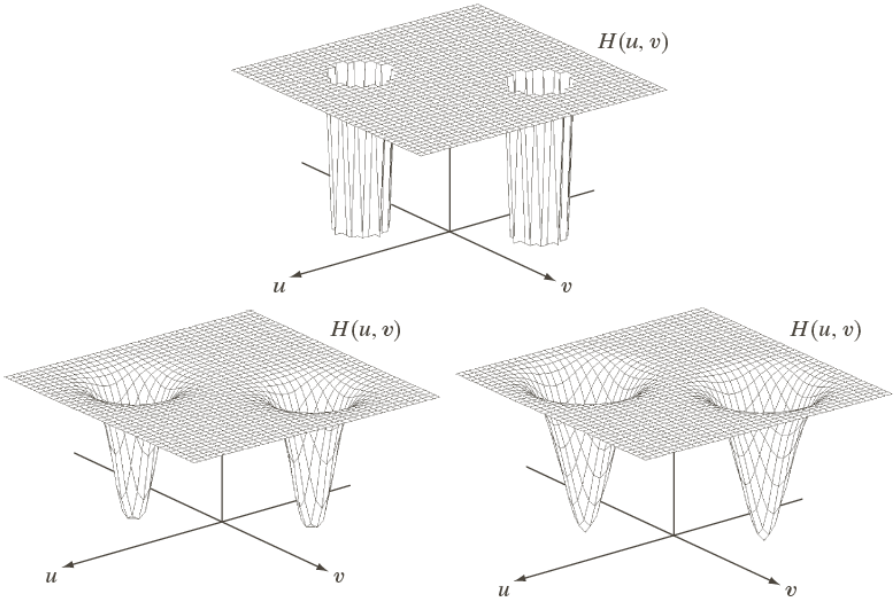

a
b c

FIGURE 5.18 Perspective plots of (a) ideal, (b) Butterworth (of order 2), and (c) Gaussian notch (reject) filters.

Similar to (5.4-1), the transfer function $H_{NP}(u,v)$ of a notch pass filter is obtained from a corresponding notch reject filter transfer function, $H_{NR}(u,v)$, by using the equation

$$H_{NP}(u,v) = 1 - H_{NR}(u,v)\,. \qquad (5.4\text{-}2)$$

Example 5.8: Removal of periodic noise by notch filtering

Figure 5.19 (a) shows the same image as Figure 4.51 (a).

Figure 5.19 (b) shows the spectrum of Figure 5.19 (a), in which the noise is not domain enough to have a clear pattern along the vertical axis.

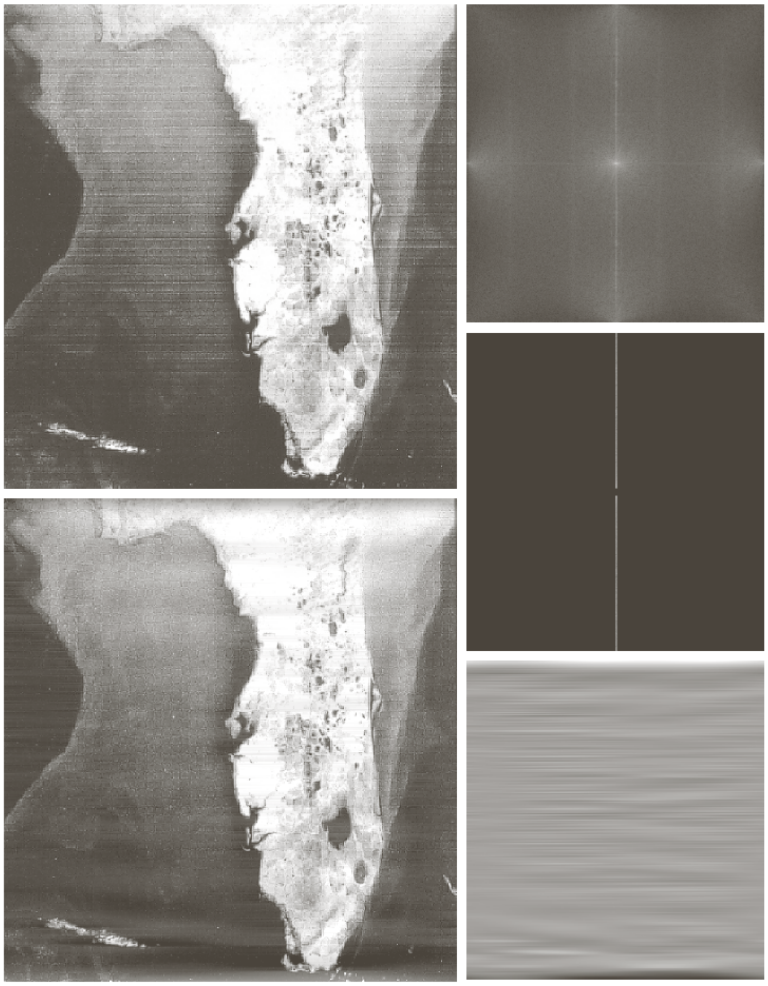

FIGURE 5.19 (a) Satellite image of Florida and the Gulf of Mexico showing horizontal scan lines. (b) Spectrum. (c) Notch pass filter superimposed on (b). (d) Spatial noise pattern. (e) Result of notch reject filtering. (Original image courtesy of NOAA.)

Figure 5.19 (c) shows the notch pass filter applied on Figure 5.19 (b).

Figure 5.19 (d) shows the spatial representation of the noise pattern (inverse transform of the notch-pass-filtered result).

Figure 5.19 (e) shows the result of processing the image with the Figure 5.19 (d) shows.

Optimum Notch Filtering

Figure 5.20 shows another example of periodic image degradation.

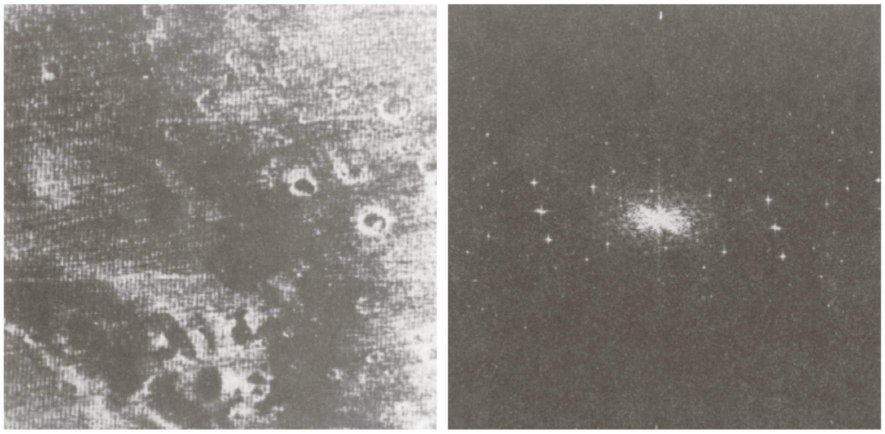

a b

FIGURE 5.20 (a) Image of the Martian terrain taken by *Mariner 6*. (b) Fourier spectrum showing periodic interference. (Courtesy of NASA.)

When several interference components are present, the methods discussed previously are not always acceptable because they may remove too much image information in the filtering process.

The method discussed here is optimum, in the sense that it minimizes local variances of the restored estimate $\widehat{f}(x,y)$.

The procedure consists of first isolating the principal contributions of the interference pattern and then subtracting a variable, weighted portion of the pattern from the corrupted image.

The first step can be done by placing a notch pass filter, $H_{NP}(u,v)$, at the location of each spike.

The Fourier transform of the interference noise pattern is given by the expression

$$N(u,v) = H_{NP}(u,v)G(u,v)\,, \qquad (5.4\text{-}3)$$

where $G(u,v)$ donates the Fourier transform of the corrupted image.

Since the formation of $H_{NP}(u,v)$ requires judgment about what is or is not an interference spike, the notch pass filter generally is constructed interactively by observing the spectrum of $G(u,v)$ on a display.

After a particular filter has been selected, the corresponding pattern in the spatial domain is obtained from the expression

$$\eta(x,y) = \mathscr{F}^{-1}\left\{H_{NP}(u,v)G(u,v)\right\}. \qquad (5.4\text{-}4)$$

Since the corrupted image is assumed to be formed by the addition of the uncorrupted image $f(x,y)$ and the interference, if $\eta(x,y)$ were known, to obtain $f(x,y)$ would be a simple matter

$$f(x,y) = \mathrm{g}(x,y) - \eta(x,y).$$

However, the filtering procedure usually yields only an approximation of the true pattern.

The effect of components not present in the estimate of $\eta(x,y)$ can be minimized by subtracting from $\mathrm{g}(x,y)$ a weighted portion of $\eta(x,y)$ to obtain an estimate of $f(x,y)$:

$$\hat{f}(x,y) = \mathrm{g}(x,y) - w(x,y)\eta(x,y), \qquad (5.4\text{-}5)$$

where the function $w(x,y)$ is called a weighted or modulation function.

One approach is to select $w(x,y)$ so that the variance of the estimate $\hat{f}(x,y)$ is minimized over a specified neighbourhood of every point (x,y).

Consider a neighbourhood of size $(2a+1)\times(2b+1)$ about a point (x,y). The local variance of $\hat{f}(x,y)$ at (x,y) can be estimated from samples, as

$$\sigma^2(x,y) = \frac{1}{(2a+1)(2b+1)} \sum_{s=-a}^{a} \sum_{t=-b}^{b} \left[\hat{f}(x+s,y+t) - \overline{\hat{f}}(x,y) \right]^2 \qquad (5.4\text{-}6)$$

where $\overline{\hat{f}}(x,y)$ is the average value of $\hat{f}(x,y)$ in the neighbourhood:

$$\overline{\hat{f}}(x,y) = \frac{1}{(2a+1)(2b+1)} \sum_{s=-a}^{a} \sum_{t=-b}^{b} \hat{f}(x+s,y+t). \qquad (5.4\text{-}7)$$

Then, we have

$$\begin{aligned}\sigma^2(x,y) = \frac{1}{(2a+1)(2b+1)} \sum_{s=-a}^{a} \sum_{t=-b}^{b} \{[&\mathrm{g}(x+s,y+t) \\ &-w(x+s,y+t)\eta(x+s,y+t)] \\ &-[\overline{\mathrm{g}}(x,y) - \overline{w(x,y)\eta(x,y)}]\}^2 \end{aligned} \qquad (5.4\text{-}8)$$

Assuming that $w(x,y)$ essentially remains constant over the neighbourhood,

$$w(x+s,y+t) = w(x,y) \qquad (5.4\text{-}9)$$

for $-a \le s \le a$ and $-b \le t \le b$. It also leads to

$$\overline{w(x,y)\eta(x,y)} = w(x,y)\overline{\eta}(x,y) \qquad (5.4\text{-}10)$$

in the neighbourhood. Then, (5.4-8) becomes

$$\begin{aligned}\sigma^2(x,y) = \frac{1}{(2a+1)(2b+1)} \sum_{s=-a}^{a} \sum_{t=-b}^{b} \{[&\mathrm{g}(x+s,y+t) \\ &-w(x,y)\eta(x+s,y+t)] \\ &-[\overline{\mathrm{g}}(x,y) - w(x,y)\overline{\eta}(x,y)]\}^2 \end{aligned} \qquad (5.4\text{-}11)$$

To minimize $\sigma^2(x,y)$, we solve

$$\frac{\partial \sigma^2(x,y)}{\partial w(x,y)} = 0 \qquad (5.4\text{-}12)$$

for $w(x,y)$. The result is

$$w(x,y) = \frac{\overline{\mathrm{g}(x,y)\eta(x,y)} - \overline{\mathrm{g}}(x,y)\overline{\eta}(x,y)}{\overline{\eta^2}(x,y) - \overline{\eta}^2(x,y)} \qquad (5.4\text{-}13)$$

Since $w(x,y)$ is assumed to be constant in a neighbourhood, it is computed for one point in each neighbourhood and then used to process all of the image points in that neighbourhood.

Example 5.9: Illustration of optimum notch filtering.

Figure 5.21 through Figure 5.23 show the result of applying the preceding techniques to the image in Figure 5.20 (a).

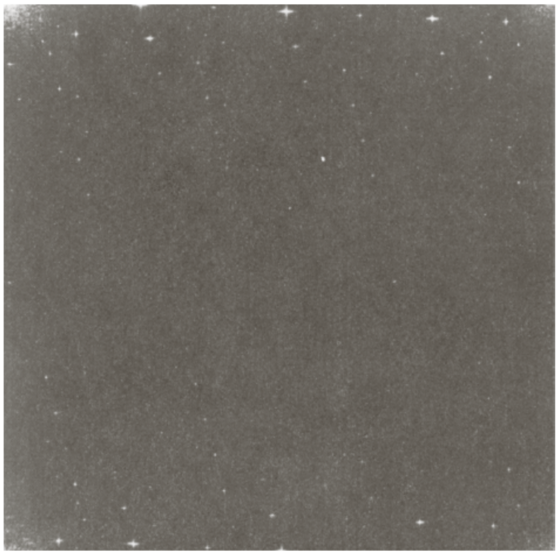

FIGURE 5.21 Fourier spectrum (without shifting) of the image shown in Fig. 5.20(a). (Courtesy of NASA.)

Figure 5.21 shows the Fourier spectrum of the corrupted image. The origin was not shifted to the center of the frequency plane in this case, so $u = v = 0$ is at the top left corner in Figure 5.21.

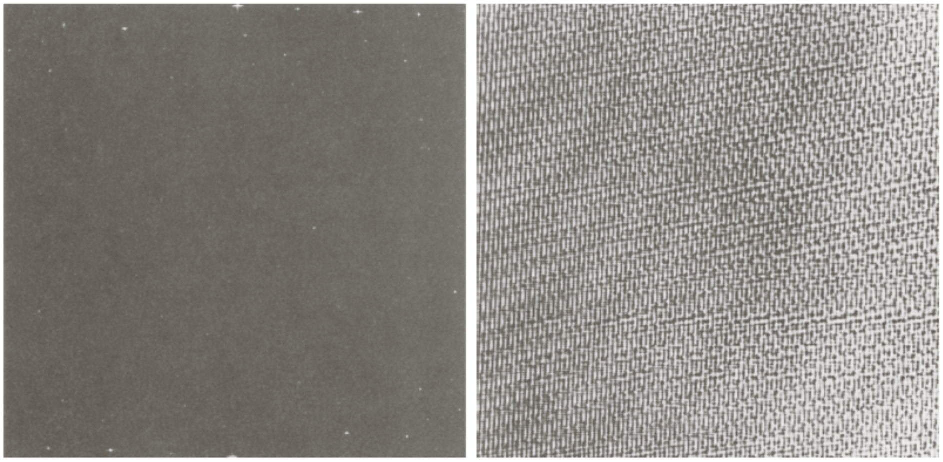

a b

FIGURE 5.22 (a) Fourier spectrum of $N(u, v)$, and (b) corresponding noise interference pattern $\eta(x, y)$. (Courtesy of NASA.)

Figure 5.22 (a) shows the spectrum of $N(u, v)$, where only the noise spikes are present.

Figure 5.22 (b) shows the interference pattern $\eta(x, y)$ obtained by taking the inverse Fourier transform of $N(u, v)$.

Note the similarity between Figure 5.22 (b) and the structure of the noise present in Figure 5.20 (a).

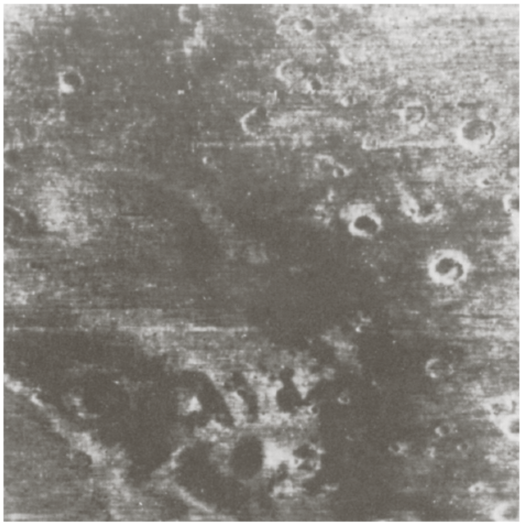

FIGURE 5.23 Processed image. (Courtesy of NASA.)

Figure 5.23 shows the processed image obtained by using

$$\hat{f}(x, y) = g(x, y) - w(x, y)\eta(x, y). \qquad (5.4\text{-}5)$$

In Figure 5.23, the periodic interference has been removed.

5.5 Linear, Position-Invariant Degradations

The input-output relationship in Figure 5.1 before the restoration can be expressed as

$$g(x,y) = H[f(x,y)] + \eta(x,y)\,. \qquad (5.5\text{-}1)$$

First, we assume that $\eta(x,y) = 0$ so that $g(x,y) = H[f(x,y)]$. H is linear if

$$H[af_1(x,y) + bf_2(x,y)] = aH[f_1(x,y)] + bH[f_2(x,y)]\,, \quad (5.5\text{-}2)$$

where a and b are scalars and $f_1(x,y)$ and $f_2(x,y)$ are any two input images. If $a = b = 1$, then (5.5-2) becomes

$$H[f_1(x,y) + f_2(x,y)] = H[f_1(x,y)] + H[f_2(x,y)]\,, \qquad (5.5\text{-}3)$$

which is called the property of additivity.

If $f_2(x,y) = 0$, (5.5-2) becomes

$$H[af_1(x,y)] = aH[f_1(x,y)]\,, \qquad (5.5\text{-}4)$$

which is called the property of homogeneity. It says that the response to a constant multiple of any input is equal to the response to that input multiplied by the same constant.

An operator having the input-output relationship

$$g(x,y) = H[f(x,y)]$$

is said to be position (space) invariant if

$$H[f(x-\alpha, y-\beta)] = g(x-\alpha, y-\beta) \qquad (5.5\text{-}5)$$

for any $f(x,y)$ and any α and β. (5.5-5) indicates that the response at any point in the image depends only on the value of the input at that point, not on its position.

With a slight change in notation in the definition of the impulse in

$$\int_{-\infty}^{\infty}\int_{-\infty}^{\infty} f(t,z)\delta(t-t_0,z-z_0)dtdz = f(t_0,z_0), \qquad (4.5\text{-}3)$$

$f(x,y)$ can be expressed as

$$f(x,y) = \int_{-\infty}^{\infty}\int_{-\infty}^{\infty} f(\alpha,\beta)\delta(x-\alpha,y-\beta)d\alpha d\beta. \qquad (5.5\text{-}6)$$

Assuming $\eta(x,y)=0$, then substituting (5.5-6) into (5.5-1) we have

$$\begin{aligned} \mathrm{g}(x,y) &= H[f(x,y)] \\ &= H\left[\int_{-\infty}^{\infty}\int_{-\infty}^{\infty} f(\alpha,\beta)\delta(x-\alpha,y-\beta)d\alpha d\beta\right]. \end{aligned} \qquad (5.5\text{-}7)$$

If H is a linear operator, then

$$\mathrm{g}(x,y) = \int_{-\infty}^{\infty}\int_{-\infty}^{\infty} H[f(\alpha,\beta)\delta(x-\alpha,y-\beta)]d\alpha d\beta. \qquad (5.5\text{-}8)$$

Since $f(\alpha,\beta)$ is independent of x and y, using the homogeneity property, it follows that

$$\mathrm{g}(x,y) = \int_{-\infty}^{\infty}\int_{-\infty}^{\infty} f(\alpha,\beta)H[\delta(x-\alpha,y-\beta)]d\alpha d\beta \qquad (5.5\text{-}9)$$

$$= \int_{-\infty}^{\infty}\int_{-\infty}^{\infty} f(\alpha,\beta)h(x,\alpha,y,\beta)d\alpha d\beta \qquad (5.5\text{-}11)$$

where the term

$$h(x,\alpha,y,\beta) = H[\delta(x-\alpha,y-\beta)] \qquad (5.5\text{-}10)$$

is called the impulse response of H.

In other words, if $\eta(x,y)=0$, then $h(x,\alpha,y,\beta)$ is the response of H to an impulse at (x,y).

Equation

$$\mathrm{g}(x,y)=\int_{-\infty}^{\infty}\int_{-\infty}^{\infty}f(\alpha,\beta)h(x,\alpha,y,\beta)d\alpha d\beta \qquad (5.5\text{-}11)$$

is called the superposition (or Fredholm) integral of the first kind, and is a fundamental result at the core of linear system theory.

If H is position invariant, from

$$H[\,f(x-\alpha,y-\beta)]=\mathrm{g}(x-\alpha,y-\beta)\,, \qquad (5.5\text{-}5)$$

we have

$$H[\,\delta(x-\alpha,y-\beta)]=h(x-\alpha,y-\beta)\,, \qquad (5.5\text{-}12)$$

and (5.5-11) reduces to

$$\mathrm{g}(x,y)=\int_{-\infty}^{\infty}\int_{-\infty}^{\infty}f(\alpha,\beta)h(x-\alpha,y-\beta)d\alpha d\beta\,. \qquad (5.5\text{-}13)$$

The expression (5.5-13) is the case of convolution integral

$$f(t)\star\,h(t)=\int_{-\infty}^{\infty}f(\tau)h(t-\tau)d\tau \qquad (4.2\text{-}20)$$

being extended to 2-D.

Equation (5.5-13) tells us that knowing the impulse of a linear system allows us to compute its response, g, to any input f. The result is simply the convolution of the impulse response and the input function.

In the presence of additive noise, (5.5-11) becomes

$$\mathrm{g}(x,y)=\int_{-\infty}^{\infty}\int_{-\infty}^{\infty}f(\alpha,\beta)h(x,\alpha,y,\beta)d\alpha d\beta+\eta(x,y)\,. \qquad (5.5\text{-}14)$$

If H is position invariant, it becomes

$$\mathrm{g}(x,y)=\int_{-\infty}^{\infty}\int_{-\infty}^{\infty}f(\alpha,\beta)h(x-\alpha,y-\beta)d\alpha d\beta+\eta(x,y)\,. \quad (5.5\text{-}15)$$

Assuming that the values of the random noise $\eta(x,y)$ are independent of position, we have

$$\mathrm{g}(x,y)=h(x,y)\bigstar\, f(x,y)+\eta(x,y)\,. \quad (5.5\text{-}16)$$

Based on the convolution theorem, we can express (5.5-16) in the frequency domain as

$$G(u,v)=H(u,v)F(u,v)+N(u,v)\,. \quad (5.5\text{-}17)$$

In summary, a linear, spatially invariant degradation system with additive noise can be modeled in the spatial domain as the convolution of the degradation function with an image, followed by the additive of noise (as expressed in (5.5-16)).

The same process can be expressed in the frequency domain as stated in (5.5-17).

5.6 Estimating the Degradation Function

There are three principal ways to estimate the degradation function used in image restoration:

Estimation by Image Observation

Suppose that we are given a degraded image without any knowledge about the degradation function H .

Based on the assumption that the image was degraded by a linear, position-invariant process, one way to estimate H is to gather information from the image itself.

In order to reduce the effect of noise, we would look for an area in which the signal content is strong.

Let the observed subimage be denoted by $g_s(x,y)$, and the processed subimage be denoted by $\hat{f}_s(x,y)$. Assuming that the effect of noise is negligible, it follows from

$$G(u,v) = H(u,v)F(u,v) + N(u,v) \qquad (5.5\text{-}17)$$

that

$$H_s(u,v) = \frac{G_s(u,v)}{\hat{F}_s(u,v)} . \qquad (5.6\text{-}1)$$

Then, we can have $H(u,v)$ based on our assumption of position invariant.

For example, suppose that a radial plot of $H_s(u,v)$ has the approximate shape of a Gaussian curve. Then we can construct a function $H(u,v)$ on a large scale, but having the same basic shape.

This estimation is a laborious process used in very specific circumstances.

Estimation by Experimentation

If equipment similar to the equipment used to acquire the degraded image is available, it is possible in principle to obtain an accurate estimate of the degradation.

Images similar to the degraded image can be acquired with various system settings until they are degraded as closely as possible to the image we wish to restore.

Then the idea is to obtain the impulse response on the degradation by imaging an impulse (small dot of light) using the same system settings.

An impulse is simulated by a bright dot of light, as bright as possible to reduce the effect of noise to negligible values. Since the Fourier transform of an impulse is a constant, it follows

$$H(u,v) = \frac{G(u,v)}{A}\,. \qquad (5.6\text{-}2)$$

Figure 5.24 shows an example.

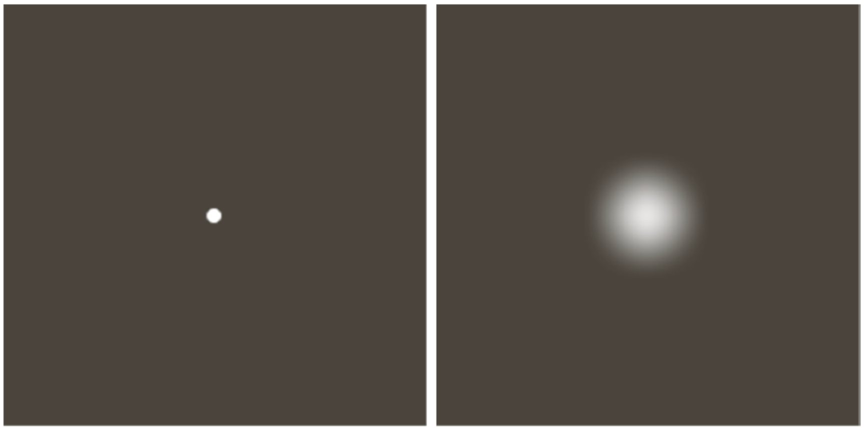

a b

FIGURE 5.24 Degradation estimation by impulse characterization. (a) An impulse of light (shown magnified). (b) Imaged (degraded) impulse.

Estimation by Modeling

Degradation modeling has been used for years.

In some cases, the model can even take into account environmental conditions that cause degradations. For example, a degradation model proposed by Hufnagel and Stanley is based on the physical characteristics of atmospheric turbulence

$$H(u,v) = e^{-k(u^2+v^2)^{5/6}}, \tag{5.6-3}$$

where k is a constant that depends on the nature of the turbulence.

Figure 5.25 shows examples of using (5.6-3) with different values of k.

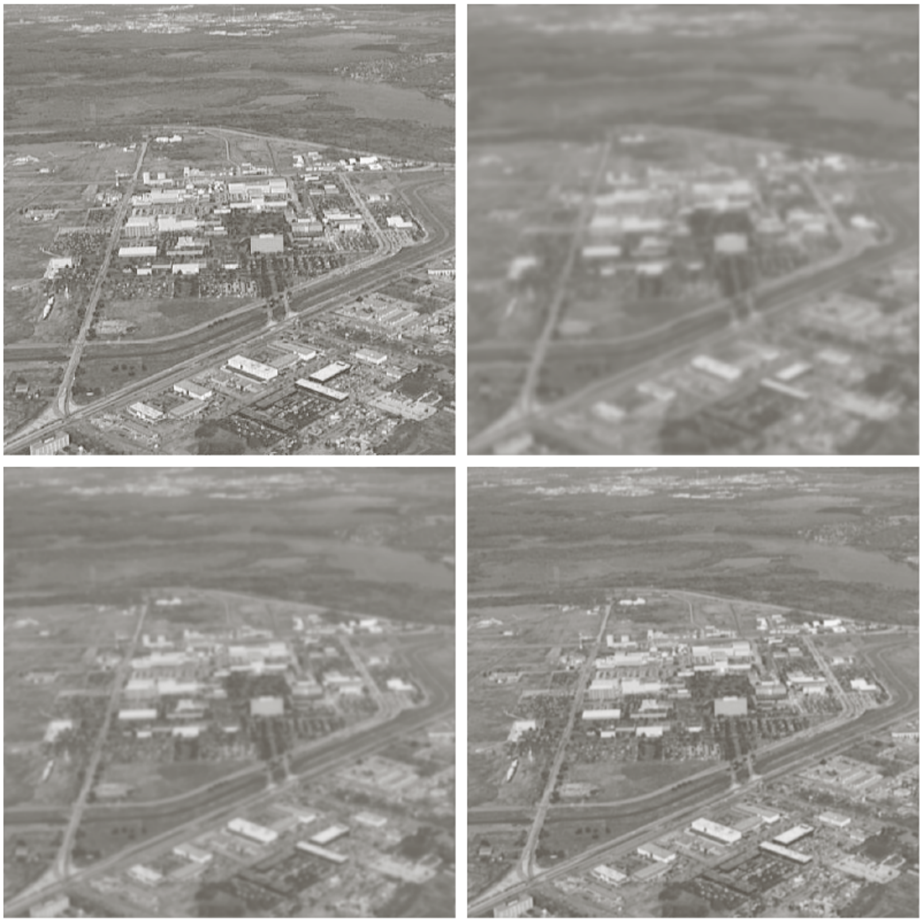

a b
c d

FIGURE 5.25 Illustration of the atmospheric turbulence model. (a) Negligible turbulence. (b) Severe turbulence, $k = 0.0025$. (c) Mild turbulence, $k = 0.001$. (d) Low turbulence, $k = 0.00025$. (Original image courtesy of NASA.)

A major approach in modeling is to derive a mathematical model starting from basic principles.

We show this procedure by a case in which an image has been blurred by uniform linear motion between the image and the sensor during image acquisition.

Suppose that an image $f(x,y)$ undergoes planar motion and that $x_0(t)$ and $y_0(t)$ are the time-varying components of motion in the x- and y- directions.

The total exposure at any point of the recording medium is obtained by integrating the instantaneous exposure over the time interval when the imaging system shutter is open.

If the T is the duration of the exposure, the blurred image $\mathrm{g}(x,y)$ is

$$\mathrm{g}(x,y) = \int_0^T f[x - x_0(t), y - y_0(t)]\,dt \,. \qquad (5.6\text{-}4)$$

From

$$F(\mu,\nu) = \int_{-\infty}^{\infty}\int_{-\infty}^{\infty} f(t,z)e^{-j2\pi(\mu t+\nu z)}dtdz \,, \qquad (4.5\text{-}7)$$

the Fourier transform of (5.6-4) is

$$\begin{aligned} G(u,v) &= \int_{-\infty}^{\infty}\int_{-\infty}^{\infty} \mathrm{g}(x,y)e^{-j2\pi(ux+vy)}dxdy \qquad (5.6\text{-}5) \\ &= \int_{-\infty}^{\infty}\int_{-\infty}^{\infty}\left[\int_0^T f[x - x_0(t), y - y_0(t)]\,dt\right]e^{-j2\pi(ux+vy)}dxdy \end{aligned}$$

By reversing the order of integration,

$$G(u,v) = \int_0^T\left[\int_{-\infty}^{\infty}\int_{-\infty}^{\infty} f[x - x_0(t), y - y_0(t)]e^{-j2\pi(ux+vy)}dxdy\right]dt$$

Since the term inside the outer brackets is the Fourier transform of the displaced function $f[x-x_0(t), y-y_0(t)]$, we have

$$\begin{aligned} G(u,v) &= \int_0^T F(u,v)e^{-j2\pi[ux_0(t)+vy_0(t)]}dt \\ &= F(u,v)\int_0^T e^{-j2\pi[ux_0(t)+vy_0(t)]}dt \end{aligned} \qquad (5.6\text{-}7)$$

By defining

$$H(u,v) = \int_0^T e^{-j2\pi[ux_0(t)+vy_0(t)]}dt \qquad (5.6\text{-}8)$$

we can rewrite (5.6-7) in the familiar form

$$G(u,v) = H(u,v)F(u,v). \qquad (5.6\text{-}9)$$

Example:

Suppose that the image in question undergoes uniform linear motion in the x-direction only, at a rate given by $x_0(t) = at/T$. When $t = T$, the image has been displaced by a total distance a. With $y_0(t) = 0$, (5.6-8) yields

$$\begin{aligned} H(u,v) &= \int_0^T e^{-j2\pi ux_0(t)}dt \\ &= \int_0^T e^{-j2\pi uat/T}dt \\ &= \frac{T}{\pi ua}\sin(\pi ua)e^{-j\pi ua} \end{aligned} \qquad (5.6\text{-}10)$$

If we allow the y-component to vary as well, with the motion given by $y_0(t) = bt/T$, the degradation function becomes

$$H(u,v) = \frac{T}{\pi(ua+vb)}\sin[\pi(ua+vb)]e^{-j\pi(ua+vb)}. \qquad (5.6\text{-}11)$$

Example 5.10: Image blurring due to motion

Figure 5.26 (b) is an image blurred by computing the Fourier transform of the image in Figure 5.26 (a), multiplying the transform by $H(u,v)$ from (5.6-11).

The parameters used in (5.6-11) were $a = b = 0.1$ and $T = 1$.

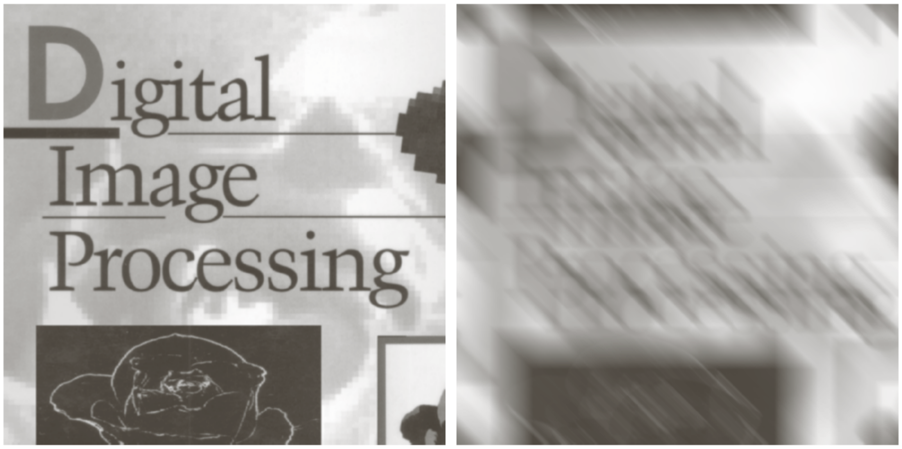

a b

FIGURE 5.26 (a) Original image. (b) Result of blurring using the function in Eq. (5.6-11) with $a = b = 0.1$ and $T = 1$.